Li-Ion Battery-Based Hybrid Diesel-Electric Railway Vehicle: In-Depth Life Cycle Cost Analysis

Josu Olmos, Iñigo Gandiaga, Dimas Lopez, Xabier Larrea, Txomin Nieva, and Iosu Aizpuru

***Abstract*—In this study, the life cycle costs of railway projects involving hybrid diesel-electric vehicles are analysed. Specifically, the analysis focuses on the comparison of 3 lithium-ion battery technologies (NMC, LTO and LFP) and 8 energy management strategies (including rule-based and optimization-based strategies). In order to develop this analysis, a methodology that returns the life cycle cost of each proposed case is presented. The methodology includes the optimization of the diesel generator and lithium-ion battery sizing. A scenario based on a real railway line is introduced, and the obtained results are compared to a traditional diesel-electric railway vehicle to develop a techno-economical discussion. The best lithium-ion battery technologies are found to be LTO and NMC, and the most appropriated strategy a state-machine controller optimised by a genetic algorithm approach. The best case obtains a life cycle cost reduction of the 4.0% and diesel savings of the 13.7% compared to a traditional diesel-electric railway vehicle. The proposed analysis is claimed to be potentially helpful for the cost-optimal design and operation definition of powertrains for hybrid railway vehicles.**

***Index Terms*—Energy management, life cycle cost analysis, optimization, lithium batteries, railway engineering.**

I. Introduction

RAILWAY is an essential transportation mode in nowadays society, both for passenger and goods [1]. Considering that the relation between the produced CO_2 emissions and the carried passenger activity is lower than in road transport, this sector becomes an important stakeholder in the path towards transport decarbonisation [2]. Even if electrified rail vehicles have been deployed for many decades, diesel powertrains remain the preferred option in many railway networks, especially in track sections where the electrification is barely cost-efficient (e.g. in low-traffic networks [3]). For instance, in Europe the 40% of the routes are not electrified yet [4], and the rate is even lower in Asia or America [5]. Consequently, it is crucial to search for cleaner alternatives in this sector.

In this context, the interest of the railway industry on integrating low-polluting technologies such as the Lithium-ion Battery (LIB) and the Fuel Cell (FC) has increased in the last years [6]–[8]. FCs have become a relevant option given the zero-emission nature of the hydrogen when obtained from renewable sources [9]. However, its cost is still roughly competitive compared to its diesel counterpart [10]. Besides, LIBs price decrease and energy/power densities increase has pushed its integration in a variety of electric vehicle applications [11], [12]. However, these improvements are not yet enough for railway vehicles solely powered by LIBs, specially when envisaged for large-range lines [13]. Regarding the current disadvantages of these low-emission solutions, hybrid railway vehicles combining a diesel generator and a LIB emerge as an alternative solution for the short and mid-term future.

When dealing with hybrid topologies, the definition of the power split ratio between the different power sources has a strong impact on the Life Cycle Costs (LCC) [14]. As that is one of its main tasks, the relevance of the Energy Management Strategy (EMS) can not be dismissed. EMSs for hybrid vehicles are typically divided into rule-based and optimization-based strategies [15]. Rule-based strategies are usually developed based on heuristics or human experience, and therefore they are causal and easy to deploy on-line. However, they do not ensure an optimal performance. They can be classified into Deterministic Rule-Based (DRB) and Fuzzy Rule-Based (FRB) strategies. DRB strategies for hybrid diesel railway vehicles have been widely proposed in the literature, including power follower [16], state-machine [17]–[19] and frequency management [3], [20] approaches. FRB strategies for hybrid diesel railway vehicles have also been proposed [21]. Regarding optimization strategies, they are based on solving the optimal power split between the power sources by means of an optimization algorithm. In Global Optimization (GOP) strategies, the optimization is developed off-line based on a pre-defined or predicted drive cycle, while in Real Time Optimization (RTOP) strategies the optimization is developed on-line. Proposed GOP strategies for hybrid diesel railway vehicles include approaches based on dynamic programming [18], [22], Pontryagin's minimum principle [17], non-linear programming [23] and genetic algorithm [24]. RTOP strategies such as equivalent consumption minimization or model predictive control have been proposed for other hybrid railway topologies such as FC vehicles [25], [26].

Manuscript received April 23, 2021; revised September 16, 2021; accepted November 14, 2021. Date of publication November 17, 2021; date of current version June 24, 2022. This work was supported in part by the BIKAINTEK Program No. 20-AF-W2-2018-00010 of the Basque Agency for Economic Development and Infrastructures. The review of this article was coordinated by Prof. Minh Cao Ta. *(Corresponding author: Josu Olmos.)*

Josu Olmos and Iñigo Gandiaga are with the Department of Energy Storage and Management, Ikerlan Technology Research Centre (Basque Research and Technology Alliance), Arrasate/Mondragon 20500, Spain (e-mail: jolmos@ikerlan.es; igandiaga@ikerlan.es).

Dimas Lopez, Xabier Larrea, and Txomin Nieva are with the Department of Product Development, CAF Power and Automation, Donostia/San Sebastian 20009, Spain (e-mail: dlopez@capower.com; xlarrea@cafpower.com; tnieva@cafpower.com).

Iosu Aizpuru is with the Department of Electronics and Computing, Faculty of Engineering, Mondragon Unibertsitatea, Arrasate/Mondragon 20500, Spain (e-mail: iaizpuru@mondragon.edu).

Digital Object Identifier 10.1109/TVT.2021.3128754

The problem of designing an optimal EMS is closed-coupled with solving the optimal sizing of the powertrain sources, as the optimal power split may vary with the hybridization level [6], [17], [20]. Besides, another issue that cannot be ignored when dealing with the integration of LIBs is the definition of its chemistry. The active materials and fabrication processes followed in the production of LIBs affect in their techno-economical characteristics, for instance voltage, internal resistance, lifetime, energy density and cost [27]. Therefore, the suitability of each LIB technology may vary depending on the requirements and use of the vehicle.

It can be concluded that when trying to reduce the LCC of hybrid diesel railway vehicles, the effect of the EMS, the LIB technology and the size of the powertrain elements cannot be neglected. Moreover, due to the identified interrelations, they should be considered in an integrated manner. Some publications have recently developed LCC analyses to reduce the cost of this application [28]–[32]. Depature and Letrouvé [28] compare the economic valorisation of a traditional diesel-electric train, a full battery train, a hydrogen train and a hybrid diesel train. They conclude that the hybrid option involves the lowest overall cost, even if it requires a higher acquisition cost compared to the traditional diesel-electric option. Besides, Cipek *et al.* [29] size the battery system of a hybrid diesel locomotive, and its performance is compared against a traditional diesel locomotive. They conclude that thanks to the hybridisation, the final cost can be reduced a 14%. Giglioli *et al.* [30] compare different topologies of a hybrid railway vehicle against a traditional diesel vehicle. They propose different sizes for the battery-based storage, and the results show that a payback time of 2 years can be obtained with some of the proposed hybrid options. Finally, Meinert *et al.* [31], [32] find that the cost of a hybrid railway vehicle can be 15% lower than in a traditional diesel vehicle. Different storage technologies are proposed and techno-economically compared. The conclusions highlight that from an economic outlook, integrating LIB technology is the best solution.

The reviewed publications [3], [16]–[24], [28]–[32], even if they partially consider some of the variables identified as crucial for the cost-efficiency of hybrid vehicles, lack of a comprehensive LCC analysis that considers integrally the effect of the EMS, LIB technology, and size of the powertrain sources. In this regard, the novelty of this study lies on the development of a LCC analysis where the influence of different EMSs and LIB technologies is examined for hybrid diesel-electric railway vehicles. For each analysed combination of EMS and LIB technology, the cost-optimal diesel generator and LIB sizes are calculated. The proposed optimization approach considers the lifespan of the LIB, calculated by means of a chemistry-dependant empirical degradation model. The proposed analysis is claimed to be potentially helpful for the cost-optimal design (technologies and size selection) and operation definition (EMS) of powertrains for hybrid diesel-electric railway vehicles.

The remainder of the paper is organized as follows. First, the models and scenario used to develop the LCC analysis are presented in Section II. Then, Section III presents the details of the different cases evaluated in the LCC sensitivity analysis (i.e. considered LIB technologies and EMSs). Section IV and Section V introduce the approaches that allow obtaining the optimal LCC value of each case being analysed, what is done by means of an optimization that returns the cost-optimal size of the powertrain elements. Finally, the obtained results are presented and techno-economically evaluated in Section VI, and the main conclusions are overviewed in Section VII.

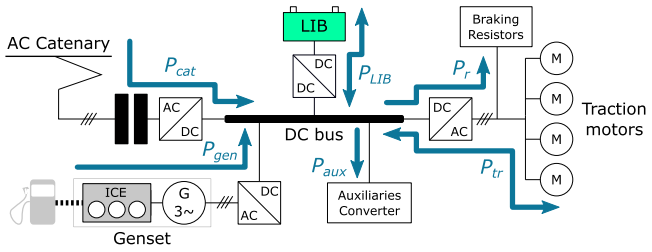

Fig. 1. H-DEMU and DEMU architectures (with and without LIB).

TABLE I
H-DEMU PARAMETERS: CAF'S CIVITY [33]

Parameter	Value	Parameter	Value
Weight [tones]	124	*Max. speed [km/h]*	210
Length [m]	86	*Traction power at wheel [kW]*	4,400

II. POWERTRAIN MODELLING

This study is focused on the railway topology denoted as bi-mode battery-based Hybrid Diesel-Electric Multiple Unit (H-DEMU). The H-DEMU can drive powered by a catenary, a diesel generator (genset) or a LIB. Fig. 1 shows the powertrain of the H-DEMU, which just adds a LIB compared to a traditional bi-mode Diesel-Electric Multiple Unit (DEMU). Table I shows representative parameters of the considered H-DEMU: the CIVITY vehicle manufactured by CAF [33].

In order to develop the LCC analysis proposed in this paper, the powertrain depicted in Fig. 1 has been modelled in MATLAB. A backward simulation model of quasi-static nature has been implemented, which is further detailed in the following subsections. Considering the scope of the current paper, a simulation step of $\Delta t = 1\ s$ has been defined [14].

A. Driving Model

The input for the simulation model consists on the power profile demanded by the traction motors (P_{tr}) and the auxiliaries converter (P_{aux}), and is defined as P_{dem}:

$$P_{dem} = P_{tr} + P_{aux} \tag{1}$$

Fig. 2 a shows the P_{dem} profile considered in the current study, which has been provided by CAF Power and Automation. $P_{dem} > 0$ represents traction demand (i.e. power has to be provided by the powertrain sources), while $P_{dem} < 0$ represents regenerated power. The depicted profile corresponds to the round trip route of the "A Coruña - A Coruña" circle railway line, which is located in the region of Galicia (Spain). The longitudinal dynamics and the traction model used to extract the power profile are not shown to ensure confidentiality. As a reference, Fig. 2 b shows the speed profile that corresponds to the P_{dem} profile.

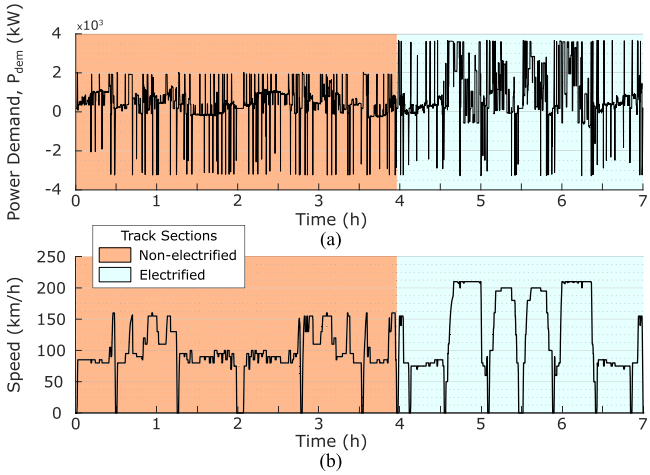

Fig. 2. Driving profile of "A Coruña - A Coruña" line: a) P_{dem} and b) Speed.

B. Power Split Model

As depicted in Fig. 2, the considered railway line consists on electrified ($E = 1$) and non-electrified ($E = 0$) sections. As in the non-electrified section the catenary is not available, the genset and LIB are in charge of satisfying P_{dem}. Besides, in the electrified section the genset is switched off, and therefore P_{dem} is divided into the catenary and LIB. In both scenarios braking resistors are activated only when regenerated power cannot be absorbed by the on-board sources:

$$P_{dem}(n) = \begin{cases} P_{gen}(n) + P_{LIB}(n) + P_r(n) & \text{for } E = 0 \\ P_{cat}(n) + P_{LIB}(n) + P_r(n) & \text{for } E = 1 \end{cases} \quad (2)$$

being P_{gen} the power provided by the genset, P_{LIB} the power given or received by the LIB, P_{cat} the power provided by the catenary, P_r the power burned in the braking resistors, and n the current time step.

In both track sections, the EMS is in charge of splitting the demand between the two sources. In this paper, different EMSs are proposed and evaluated for the non-electrified section. More detail about these EMSs is given in Section III-B. Besides, in the case of the electrified section a simple rule-based strategy is proposed. In order to reduce the LIB degradation, the catenary gives all the traction demand ($P_{dem} > 0$), while the LIB is charged with the regenerative power ($P_{dem} < 0$). Additionally, if this energy is not enough for the LIB to recover its initial State-of-Charge (SOC) at the end of the trip, the catenary provides additional power to charge the LIB.

C. Genset Model

The genset model returns the diesel consumption (l_f) for each time step, based on the required P_{gen} and the efficiency curve depicted in Fig. 3. The curve has been obtained extracting an optimal path from the efficiency map of the genset [14]. As further explained in Section IV and V, in this paper different genset sizes are evaluated. For each size, the efficiency curve is proportionally scaled.

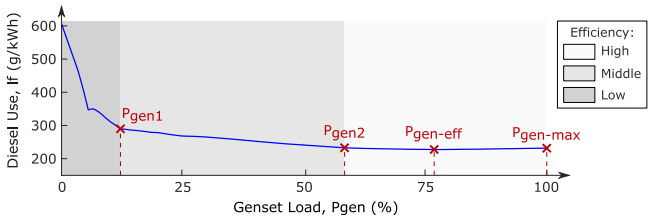

Fig. 3. Genset efficiency curve.

D. Model

LIB Model: The LIB model is based on an equivalent circuit composed of an open-circuit voltage source (V_{oc}) connected in series with an internal resistance (R_{int}). Both V_{oc} and R_{int} are defined as non-linear functions of the SOC [14]. At each discrete time step n, the LIB current (I_{LIB}) and SOC are calculated:

$$I_{LIB}(n) = \frac{V_{oc}(n) - \sqrt{V_{oc}(n) - 4 \cdot R_{int}(n) \cdot P_{LIB}(n)}}{2 \cdot R_{int}(n)} \quad (3)$$

$$SOC(n) = SOC(n-1) - \left(I_{LIB}(n) \cdot \frac{\Delta t}{Q} \right) \cdot 100 \quad (4)$$

being Q the current battery capacity.

In the used commitment, a positive I_{LIB} denotes that the LIB is discharging. I_{LIB} is limited depending on the maximum charge and discharge C-rates (C_{ch} and C_{dch}), defined as $C = I_{LIB}/Q$. Besides, Q can be updated at any time of the LIB lifetime based on its State-of-Health (SOH), which is defined as $SOH = Q/Q_0$ (Q_0 refers to the initial or nominal LIB capacity). All the introduced LIB parameters may vary depending on the chemistry and size being analysed, as it is further detailed in Sections III, IV, and V.

E. Catenary Model

Being the scope of this study the analysis of the non-electrified section, the AC catenary is modelled as a linear system in which the electricity consumption (e_{cat}) is calculated based on an average transmission efficiency factor ($\gamma = 90\%$):

$$e_{cat}(n) = \frac{P_{cat}(n) \cdot \Delta t}{\gamma} \quad (5)$$

F. Converters Model

As the scope of this study is more oriented to the power and energy analysis of the H-DEMU operation, the converters of the powertrain are modelled with a fixed average efficiency value ($\eta_{conv} = 95\%$).

III. Overview of Sensitivity Analysis

As introduced in previous sections, the main contribution of this paper consists on evaluating the influence of different LIB technologies and EMSs on the LCC of H-DEMUs. This approach is developed by means of a sensitivity analysis, in which the LCC variation when using different LIB technologies and

TABLE II
PARAMETERS OF CONSIDERED LIB CHEMISTRIES (CELL-LEVEL)

	LFP	NMC	LTO
Nominal capacity [Ah]	28	46	23
Nominal cell voltage [V]	3.2	3.7	2.3
Max. C_{ch} / C_{dch} *[C]*	4.0 / 6.5	3.0 / 5.0	4.0 / 4.5
Calendar Life [years]	10	15	20
Cycle Life (@80%DOD) [cycles]	4,400	4,800	24,200
Specific Energy (@pack-level) [Wh/kg]	48.0	86.9	53.3
Energy Density (@pack-level) [Wh/L]	81.1	122.2	52.8

EMSs is calculated. In the following paragraphs, the analysed LIB technologies and EMSs are introduced.

A. LIB Technologies

Different LIB technologies exist depending on the deployed anode and cathode material. In the current study the following chemistries are considered (cathode/anode): Lithium Iron Phosphate/Graphite (LFP/G), Lithium Nickel Manganese Cobalt Oxide/Graphite (NMC/G) and Lithium NMC/Titanate (NMC/LTO). For the sake of simplicity, in the remainder these technologies will be referred as LFP, NMC and LTO, respectively. As Table II outlines, the characteristics of these chemistries may differ (LIB lifespans come from [34]), what evidences the importance of the proposed approach.

B. Energy Management Strategies

In the present study 4 DRB, one FRB and 3 GOP strategies are proposed, which are presented in the following paragraphs. It is worth to point out that the rule based strategies have been designed considering the efficiency curve of the genset (Fig. 3), specifically the operation points P_{gen1} (low limit of middle efficiency zone), P_{gen2} (low limit of high efficiency zone), $P_{gen-eff}$ (point of maximum efficiency) and $P_{gen-max}$ (maximum power point). Besides, for all strategies the LIB operation window is defined between 20-90% SOC (SOC_{min} and SOC_{max} values, respectively).

1) DRB – Power Follower (PF): In this approach a constant P_{gen} is defined for the genset. Therefore, the LIB works as a buffer, giving or absorbing power depending on the difference between the genset reference and the instantaneous demand (Fig. 4 a). In case the LIB cannot provide the required power peak, the genset works at maximum load. Besides, if the LIB cannot absorb all the peak, the working point of the genset is reduced. Depending on where is the genset reference fixed, the strategy will be oriented to sustain or deplete the LIB charge. In this study, $P_{gen-eff}$ is defined as the genset reference, allowing a high efficiency genset operation and defining a strategy more oriented to sustain the LIB charge.

2) DRB – Improved Power Follower for Charge Sustaining (IPF-CS): This approach is partially based on the PF strategy. In this case, the genset operation is extended to more points, but maintaining them on the high efficiency zone (right part of Fig. 3). Indeed, the efficiency loss when turning from $P_{gen-eff}$ to P_{gen2} or $P_{gen-max}$ is almost negligible. As Fig. 4 b shows, the genset works at full load when the demand is higher than

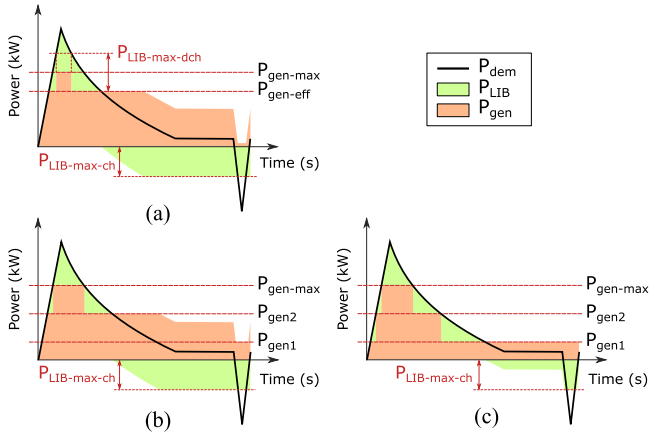

Fig. 4. DRB strategies: a) Power Follower b) Improved Power Follower for Charge Sustaining c) Improved Power Follower for Charge Depleting.

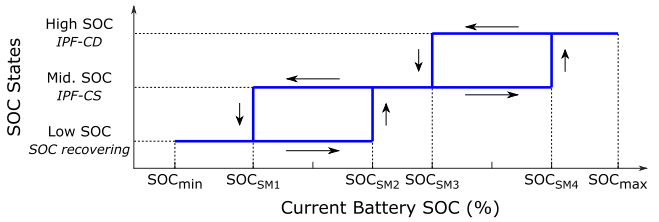

Fig. 5. Working principle of State Machine strategy.

$P_{gen-max}$, and on P_{gen2} in the rest of cases (except if that involves overcharging the LIB, in that case the genset is allowed to work on the middle efficiency zone).

3) DRB – Improved Power Follower for Charge Depleting (IPF-CD): This strategy is an extension of IPF-CS, but in this case the genset is allowed to work in normal conditions on the middle efficiency zone (central part of Fig. 3). Therefore, as Fig. 4 c shows, when the demand is lower than P_{gen2}, the genset works at P_{gen1}. Compared to IPF-CS, this strategy asks more energy to the LIB, so it may realize a deeper cycle.

4) DRB – State Machine (SM): In order to combine the characteristics and avoid the disadvantages of IPF-CS and IPF-CD strategies (high diesel use and fast discharge of the LIB, respectively), a strategy based on a state machine controller is proposed. Depending on the SOC of the LIB, three different states are defined: at high SOC, IPF-CD strategy is deployed to exploit the available energy on the LIB; at middle SOC, IPF-CS strategy is deployed to maintain the charge of the LIB; and at low SOC, the genset works at full load in order to recover the charge and avoid a full discharge of the LIB. Fig. 5 shows the working principle of the SM strategy. Values SOC_{SM1} to SOC_{SM4} are defined as 50%, 60%, 70% and 80%, respectively.

5) FRB – Fuzzy Logic-Based Strategy (FL): The proposed strategy is based on the FL controller developed by López-Ibarra *et al.* for a plug-in hybrid bus [35], which has been adapted for the current application. Fig. 6 depicts the designed membership functions for the three control variables: SOC of the LIB, power demand (P_{dem}), and genset power in the previous time step (P_{gen}). 4 membership functions are defined for SOC variable

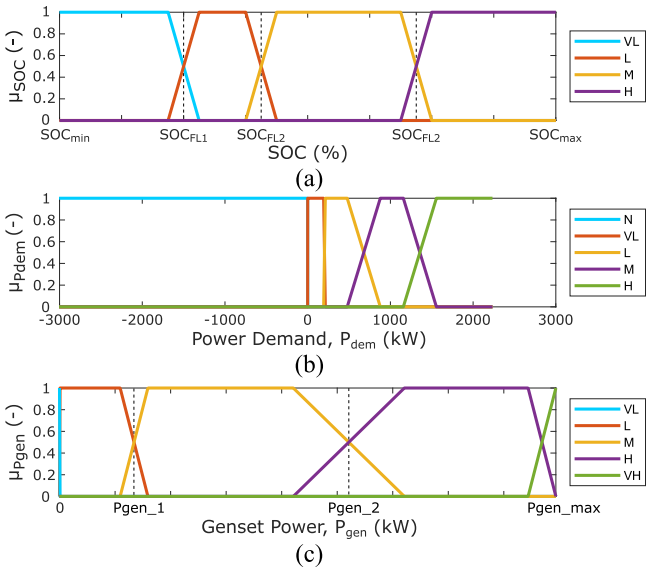

Fig. 6. Membership functions of Fuzzy Logic Strategy: a) LIB state of charge b) Power demand at DC bus c) Genset operation point. (N: Negative, VL: Very Low, L: Low, M: Middle, H: High, VH: Very High).

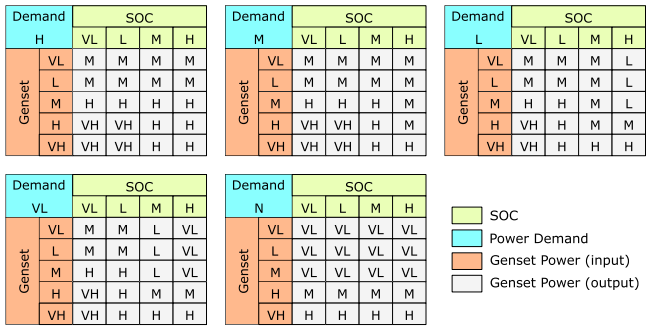

Fig. 7. Rules of Fuzzy Logic Strategy (N: Negative, VL: Very Low, L: Low, M: Middle, H: High, VH: Very High).

(VL: Very Low, L: Low, M: Middle, and H: High) according to the thresholds SOC_{FL1}, SOC_{FL2} and SOC_{FL3} (defined as 30%, 42.5% and 67.5%, respectively). Regarding P_{dem}, the membership functions are designed to represent a negative demand for regenerative braking (N: Negative), a low demand value required by the auxiliaries (VL), a demand lower than 1/3 of the power peak (L), a demand lower than 2/3 of the peak (M) and a demand around the peak (H). Finally, for P_{gen} 5 membership functions are defined, which represent an idle operation (VL), an operation on the low efficiency zone (L), middle efficiency zone (M), high efficiency zone (H) and around the maximum load (VH: Very High). Fig. 7 summarizes the set of rules defined for the controller. As seen, the output variable is the power of the genset in the current time step, so it involves the same membership functions as in Fig. 6 c.

6) GOP – Optimized State Machine (GA-SM): In this case, the SM strategy introduced in point (4) is optimized by means of a Genetic Algorithm (GA) optimization approach. Specifically, the SOC thresholds SOC_{SM1}, SOC_{SM2}, SOC_{SM3} and SOC_{SM4} (Fig. 5) are set as optimization variables, instead of being defined based on previous experience (as done in SM strategy). Further information regarding the GA optimization is given in Section IV.

7) GOP – Optimized Fuzzy Logic-Based Strategy (GA-FL): In this approach, the FL strategy introduced in point (5) is optimized by means of a GA optimization approach. Thresholds SOC_{FL1}, SOC_{FL2} and SOC_{FL3} are set as optimization variables (Fig. 6 a). Further information is given in Section IV.

8) GOP – Dynamic Programing (DP): This global optimization is based on an algorithm that calculates the optimal split factor (in terms of fuel consumption) between the genset and LIB for each time step, based on Bellman's optimality principle. The resulting operation is characterized by frequent switches in the power split factor, what further complicates its on-line implementation. Therefore, DP is commonly used just as baseline for benchmarking other EMSs [22]. The optimization problem is based on the following cost function:

$$J = \sum_{n=0}^{N-1} l_f\left(U(n)\right) \cdot \Delta t \tag{6}$$

where l_f refers to the fuel mass consumption at each time step Δt, determined by the power split factor U, within the route length N. The DP algorithm integrated in the current study is based on the function developed in [36].

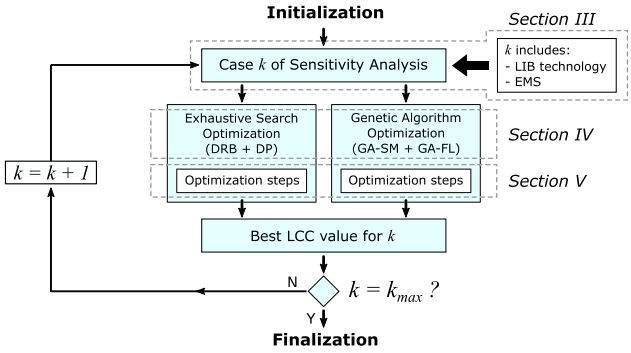

Fig. 8. Overview of sensitivity analysis, including two optimization approaches to obtain the LCC values: exhaustive search and genetic algorithms.

IV. Optimization Methodology

As previously explained, for each case of the sensitivity analysis the cost-optimal combination of genset and LIB size is calculated. This section presents the methodology followed to develop this optimization.

In order to understand the methodology, Fig. 8 shows an overview of the process followed for the development of the sensitivity analysis. The aim is to obtain the LCC value of each case to be analysed ($k \in k_{max}$). At each k a certain combination of LIB technology and EMS is evaluated. The LCC of each case k is obtained by means of an optimization that returns the cost-optimal combination of installed LIB modules (n_{LIB}) and number of gensets (n_{gen}). Additionally, the initial SOC value of

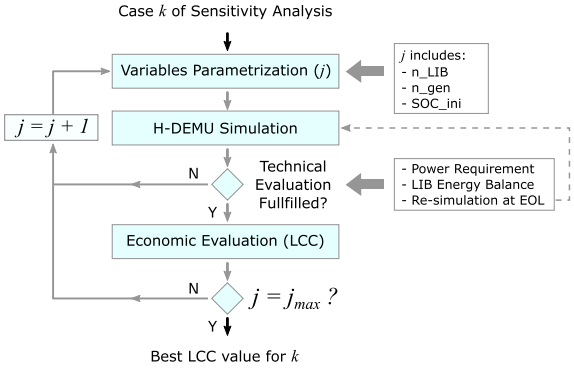

Fig. 9. Optimization by exhaustive search (DRB and DP strategies).

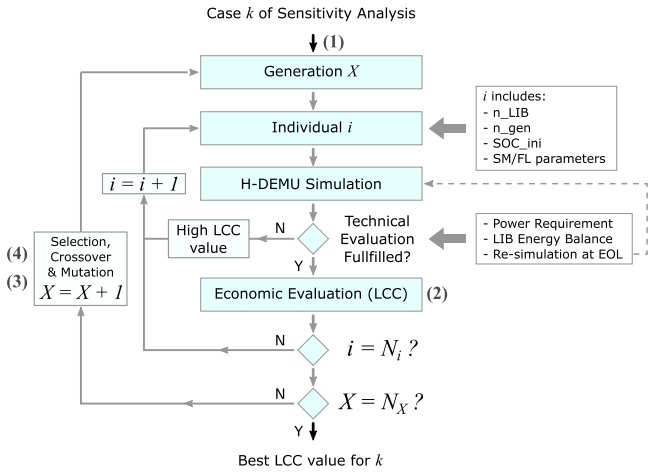

Fig. 10. Optimization by Genetic Algorithm (GA-SM and GA-FL strategies).

the LIB (SOC_{ini}) is also optimised, as it is understood to be a key variable for the EMS performance.

The deployed optimization methodology differs depending on the strategy being analysed. On the one hand, when analysing rule-based and DP strategies, an exhaustive search is proposed to solve the optimization. On the other hand, in the case of GA-SM and GA-FL strategies, the parameters related to the EMS are also optimised (see Section III-B). Due to the increased number of variables, the implementation of an exhaustive search becomes impracticable. Therefore, a GA based optimization approach is proposed. In the following subsections the two optimization methodologies are introduced.

A. Optimization Approach A: Exhaustive Search

The optimization by exhaustive search consists on an iterative sequence composed of four steps, in which all the range of feasible solutions ($j \in j_{max}$) is assessed one by one. The main steps are depicted in Fig. 9 and further detailed in Section V.

B. Optimization Approach B: Genetic Algorithm

The GA is a heuristic optimization solving method based on the concept of natural selection [14]. The algorithm repeatedly modifies a population of individuals (i). Each i includes a certain combination of optimization variables. At each step, the GA selects the best individuals from the current population to be parents and uses them to produce children, trying to keep the best features for the next generation (X). In short, it consists of an iterative process through several phases, as Fig. 10 shows: (1) a random initial population of N_i individuals is generated, (2) each individual is evaluated according to a fitness function, which in the current approach is the LCC value (the main steps for its calculation are detailed in Section V), (3) the best individuals are selected to join the next generation, and (4) new individuals are generated by means of crossover and mutation approaches. Steps (2)-(4) are repeated until a desired number of generations (N_X) is reached.

V. LCC Calculation Approach

In this section the main steps of the optimization approaches presented in Section IV are explained in detail. Indeed, these steps are followed to obtain the LCC value or optimization cost function of each case being evaluated by the algorithm (either exhaustive search or GA). *Variables Parametrization* in Fig. 9 and *Individual i* in Fig. 10 are in fact the same step, so they are introduced together.

TABLE III
Optimization Variables and Defined Bounds

Variable		Bounds		Optimization Approach
$n_{LIB}(j/i)$	$\in$	$\{0, 1, \dots N_{LIB}\}$	[-]	Exhaustive Search, GA
$n_{gen}(j/i)$	$\in$	$\{0, 1, \dots N_{gen}\}$	[-]	Exhaustive Search, GA
$SOC_{ini}(j/i)$	$\in$	$\{20 - 90\}$	[%]	Exhaustive Search, GA
$SOC_{SMX}(i)$	$\in$	$\{20 - 90\}$	[%]	GA (only in GA-SM)
$SOC_{FLX}(i)$	$\in$	$\{20 - 90\}$	[%]	GA (only in GA-FL)

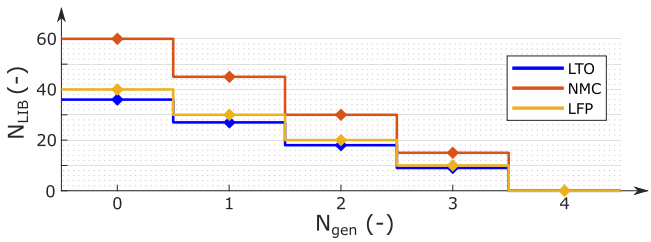

Fig. 11. Relation between N_{gen} and N_{LIB} for LTO, NMC, and LFP.

A. Variables/Individuals Parametrization

Table III shows the bounds of the variables that compose j and i (due to their similarities, SOC_x values of GA-SM and GA-FL strategies are represented as a single variable). N_{LIB} and N_{gen} define the maximum number of LIB modules and gensets, respectively. Each LIB module is constructed connecting cells in series and parallel to reach a nominal energy of 20 kWh, and each genset has a nominal power of 500 kW. Due to space limitations on the H-DEMU, N_{LIB} changes with respect to N_{gen} (i.e. if more gensets are integrated, less space is available for the LIB modules). In addition, N_{LIB} also varies with respect to the LIB technology, as the energy densities differ (Table II). Fig. 11 shows the relation between N_{LIB} and N_{gen} for the three LIB chemistries. It is also worth to point out that SOC_{ini} is a continuous variable in the GA approach, and an integer variable

in the exhaustive search (steps of 10% SOC are defined to reduce computation time).

B. H-DEMU Simulation Model

The performance of the H-DEMU is evaluated by means of the simulation model introduced in Section II. It is worth to mention that at this step, LIB characteristics (Q and R_{int}) are set at Beginning-of-Life (BOL) values (nominal values).

C. Technical Evaluation

Simulation results are technically evaluated considering aspects of power requirement (demand must be fulfilled at each time step) and LIB energy balance ($SOC_{end} \geq SOC_{ini}$). The second constraint is necessary so the results of a single simulation can be extrapolated to the whole H-DEMU life (which is required for the economic evaluation step). Then, the simulation is repeated with the LIB characteristics set at End-of-Life (EOL) values (Q at 80% and R_{int} at 150% of the BOL or nominal values). Iteration j or individual i is considered feasible and its LCC is calculated only if the technical aspects are met in both simulations (BOL and EOL).

D. Economic Evaluation (LCC Model)

The cost model returns the LCC value of each feasible solution, which corresponds to the minimization function of both optimization approaches. The model considers the costs of the whole H-DEMU lifetime, divided into acquisition (C_{acq}), operation (C_{op}) and maintenance costs (C_{maint}):

$$LCC(i/j) = C_{acq}(i/j) + C_{op}(i/j) + C_{maint} \tag{7}$$

1) Acquisition Cost (C_{acq}): The first term includes the initial costs of the LIB, genset and the rest of the train.

$$C_{acq}(i/j) = C_{tr} + c_{LIB} \cdot n_{LIB}(i/j) + c_{gen} \cdot n_{gen}(i/j) \tag{8}$$

being C_{tr} the cost of the train without LIB and genset, c_{LIB} the referential cost per module of the LIB technology, and c_{gen} the referential cost of a single genset.

2) Operation Cost (C_{op}): This term includes the costs related to the diesel fuel consumption (C_f), electricity consumption from catenary (C_{cat}) and LIB replacements (C_{repl}):

$$C_{op}(i/j) = C_f(i/j) + C_{cat}(i/j) + C_{repl}(i/j) \tag{9}$$

On the one hand, the costs related to the fuel and electricity use are calculated annualizing the daily consumptions:

$$C_f(i/j) = \sum_{y=1}^{Y} (L_f(i/j) \cdot c_f) \cdot t_{op} \cdot (1+I)^{-y} \tag{10}$$

$$C_{cat}(i/j) = \sum_{y=1}^{Y} (E_{cat}(i/j) \cdot c_{cat}) \cdot t_{op} \cdot (1+I)^{-y} \tag{11}$$

being L_f the daily diesel consumption, c_f the referential fuel cost, E_{cat} the daily electricity consumption, c_{cat} the referential electricity cost, t_{op} the number of operation days per year, I the discount rate, y the current year, and Y the service life. To calculate L_f and E_{cat}, a number of round trips per day is defined according to the H-DEMU daily operation time (t_{day}).

TABLE IV
PARAMETERS FOR CHEMISTRY DEPENDANT DEGRADATION MODEL [27]

	α	β	k_1	k_2	k_3	k_4	k_5	k_6	k_7
LTO	0.80	0.0032	16.8	293	-0.005	0.01	0.01	0	0
NMC	0.92	0.0017	21.7	293	0.022	0.26	0.16	-0.02	42
LFP	0.87	0.0034	5.88	293	-0.005	0.10	0.30	0.05	42

On the other hand, the cost related to the LIB replacements is obtained as follows:

$$C_{repl}(i/j) = \sum_{r=1}^{R(i/j)} c_{LIB} \cdot n_{LIB}(i/j) \cdot (1+I)^{-r \cdot y_r(i/j)} \tag{12}$$

being R the total LIB replacements, y_r the estimated LIB lifetime, and r the number of the current LIB replacement.

The value y_r is obtained based on the empirical degradation model developed by Olmos *et al.* in [27]. The LIB lifespan is typically defined as the moment when the SOH drops to the 80%, i.e. the LIB has lost 20% of its initial capacity (Q_0). The capacity loss is caused by the cycling ageing (produced by the use of the LIB) and the calendar ageing (produced inevitably by the course of time) [27]. Therefore, the capacity decay (ΔSOH) can be divided into the cycling capacity loss (ΔSOH_{cyc}) and calendar capacity loss (ΔSOH_{cal}):

$$\Delta SOH(FEC, t) = \Delta SOH_{cyc}(FEC) + \Delta SOH_{cal}(t) \tag{13}$$

ΔSOH_{cal} is defined as a linear capacity decay over time t (following calendar life data given in Table II) and ΔSOH_{cyc} is defined as a power-based capacity decay over FEC (number of full equivalent cycles), as depicted in (14):

$$\Delta SOH_{cyc} = \delta \cdot FEC^{\alpha} \tag{14}$$

being δ the degradation rate and α the degradation rate factor.

Value δ is affected by the typical cycling degradation factors: temperature (T), depth-of-discharge (DOD), charge and discharge currents (C_{ch} and C_{dch}) and middle SOC ($mSOC$). According to [27], δ can be deduced by (15):

$$\delta = \beta \cdot exp\left(k_1 \cdot \frac{T - k_2}{T} + k_3 \cdot DOD + k_4 \cdot C_{ch} + k_5 \cdot C_{dch}\right) \cdot \left[1 + k_6 \cdot mSOC \cdot \left(1 - \frac{mSOC}{k_7}\right)\right] \tag{15}$$

where β, k_1, k_2, k_3, k_4, k_5 and k_7 are the parameters relating the degradation rate and the degradation factors. Authors in [27] obtain all the parameters of (14) and (15) for LFP and NMC chemistries. Additionally, parameters for LTO have been obtained following the same methodology and data provided in that publication. All the parameters are given in Table IV.

In order to obtain the value y_r, equations (13)-(15) are called repeatedly until ΔSOH equals 20%. This requires to extract variables $FEC, T, DOD, C_{ch}, C_{dch}$ and $mSOC$ from the cycle realized by the LIB at each simulation time step. C_{ch} and C_{dch}

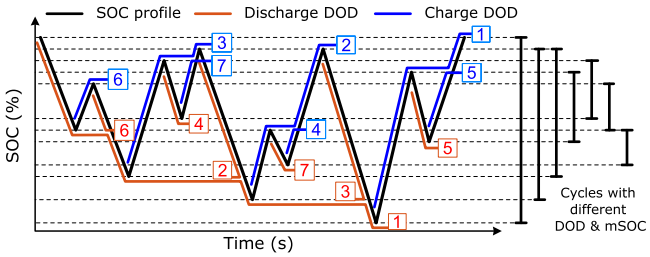

Fig. 12. Rainflow algorithm working principle [14].

TABLE V
CONSIDERED ECONOMIC PARAMETERS

Parameter	Value	Ref.	Parameter	Value	Ref.
t_{day} [h/day]	15	-	c_{LIB} - LTO [€/kWh]	1500	[37]
t_{op} [days/year]	320	-	c_{LIB} - NMC [€/kWh]	800	[37]
Y [years]	30	-	c_{LIB} - LFP [€/kWh]	1200	[5]
I [%]	2.5	-	c_f [€/L]	1.1	[38]
c_{gen} [€/kW]	500	[5]	c_{cat} [€/kWh]	0.06	[4]

are directly related to I_{LIB}, FEC is obtained by the Coulomb counting method (integration of I_{LIB} over t), and DOD and $mSOC$ are obtained by the Rainflow algorithm. This algorithm, depicted in Fig. 12, analyses the SOC profile from simulation and extracts all the realized cycles (for further information see [14]). A constant T of 20°C is defined assuming a correct operation of the cooling system.

3) Maintenance Cost (C_{maint}): This term includes the costs related to the maintenance of the H-DEMU. An average value for the cost per year is defined and then annualized.

$$C_{maint} = \sum_{y=1}^{Y} c_{maint} \cdot (1+I)^{-y} \tag{16}$$

being c_{maint} the average maintenance cost in a year.

VI. RESULTS AND DISCUSSION

In this section the results of the sensitivity analysis are presented, and a discussion is carried out focusing on the sizing, LIB technologies and strategies comparison. Table V shows the considered economic parameters, which have been defined following previous literature [4], [5], [37], [38]. Parameters without a reference refer to own assumptions. The obtained results are presented in Fig. 13 and Table VI. On the one hand, Fig. 13 shows the LCC of each proposed case, divided into the terms of (7) and (9). On the other hand, Table VI further extends these results, showing the LCC, diesel consumption (L_f), optimal sizing values (n_{LIB} and n_{gen}), LIB lifespan estimation (y_r) and number of LIB replacements (R) of each case. LCC and L_f are given in per unit (p.u.) values in relation to the results of a DEMU, which was simulated in the same route and conditions. The most relevant values are highlighted.

In the following subsections, in order to ease the analysis of the obtained results, the discussion is divided into the comparison of LIB technologies, the comparison of the different strategies, and the analysis of the optimal sizing results.

TABLE VI
SUMMARY OF RESULTS

EMS	LIB	LCC [p.u.]	L_f [p.u.]	n_gen [kW]	n_LIB [kWh]	y_r [years]	R [-]
DEMU	-	1	1	2000	-	-	-
PF	LTO	0.996	0.965	1000	280	10.29	2
	NMC	1.016	0.993	1500	280	5.32	5
	LFP	1.052	0.990	1500	200	2.38	12
IPF-CS	LTO	**0.965**	**0.884**	1000	300	12.55	2
	NMC	**0.973**	**0.884**	1000	480	7.91	3
	LFP	1.009	0.971	1500	200	4.83	6
IPF-CD	LTO	N.f.s.	N.f.s.	N.f.s.	N.f.s.	N.f.s.	N.f.s.
	NMC	N.f.s.	N.f.s.	N.f.s.	N.f.s.	N.f.s.	N.f.s.
	LFP	N.f.s.	N.f.s.	N.f.s.	N.f.s.	N.f.s.	N.f.s.
SM	LTO	**0.970**	**0.881**	1000	360	13.24	2
	NMC	**0.971**	**0.869**	1000	540	8.58	3
	LFP	1.013	0.934	1500	200	3.25	9
FL	LTO	0.967	0.868	1000	360	12.14	2
	NMC	0.976	0.896	1500	300	6.49	4
	LFP	1.054	0.851	1000	400	2.61	11
GA-SM	LTO	**0.960**	**0.863**	1000	320	12.67	2
	NMC	**0.966**	**0.848**	1000	580	8.81	3
	LFP	1.003	0.949	1500	200	4.42	6
GA-FL	LTO	0.967	0.874	1000	340	12.34	2
	NMC	0.972	0.857	1000	600	8.59	3
	LFP	1.033	0.943	1500	180	3.10	13
DP	LTO	**0.948**	**0.813**	1000	360	11.75	2
	NMC	**0.953**	**0.743**	1000	600	6.13	4
	LFP	1.043	0.792	1000	400	2.45	12

A. Analysis of LIB Technologies

The first conclusion when looking to the obtained results is that when hybridizing a traditional DEMU the cost-effectiveness depends on the integrated LIB technology. In general, LTO and NMC technologies obtain a LCC lower than the traditional DEMU, with a maximum reduction of the 5.2% and 4.7%, respectively. However, LFP is not able to improve the result of the DEMU in any case, what demonstrates that it is not an appropriate technology to be integrated in the proposed application, at least from the LCC point of view. The main cause is the shorter life of this technology compared to NMC and LTO. As it can be seen in Table VI, LFP batteries always require more than 6 replacements, and in some cases that value is even doubled. When looking to Fig. 13, it can be also checked that the cost related to the LIB replacements is too high in many LFP cases (e.g. in PF, FL, GA-FL and DP). And even in the cases when the strategy is able to reduce the degradation (e.g. in IPF-CS, SM and GA-SM), it involves a high diesel consumption compared to the other technologies, what inevitably makes the LCC be always high.

Related to the results of NMC and LTO, it can be stated that in general the difference between both technologies is low. However, the results of LTO are always better: the LCC is 2.0% lower in PF, 0.8% lower in IPF-CS, 0.1% lower in SM, 0.9% lower in FL, 0.6% lower in GA-SM, and 0.5% lower in GA-FL and DP. Even if in general NMC obtains a lower diesel use (as it can integrate a bigger LIB), the final cost is compensated in LTO due to the lower replacements cost.

Therefore, two conclusions have been obtained when looking to the results of the LIB technologies. On the one hand, it has

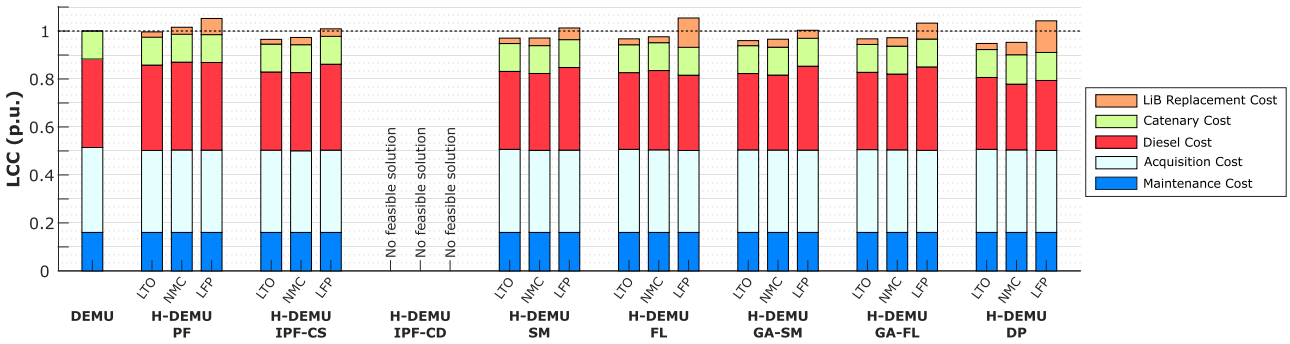

Fig. 13. LCC Results for the different EMS and LIB technologies.

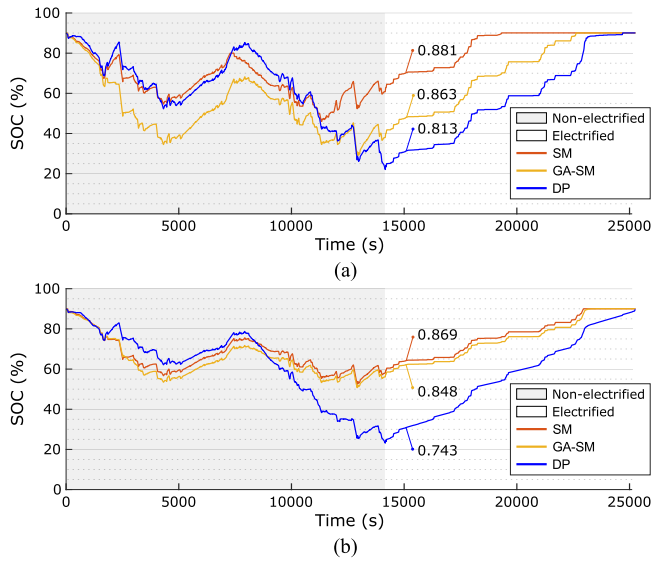

Fig. 14. SOC in representative cases: (a) for LTO technology (b) for NMC technology. Numeric points represent diesel consumptions (L_f, in p.u.).

been highlighted that LTO and NMC are the most appropriated technologies for the proposed scenario, with LTO obtaining slightly better results. On the other hand, it has been concluded that when comparing the results of the different technologies, the cost of the required replacements becomes the most important term of the LCC.

B. Analysis of EMSs

Simulation results of some representative cases are shown in Fig. 14 to ease the discussions of this section. Indeed, the SOC profile is depicted for SM, GA-SM and DP strategies.

At a first look to the results (Fig. 13 and Table VI), it can be checked that in IPF-CD strategy no feasible solutions are obtained. The reason is that the technical evaluation is not fulfilled in any combination of genset and LIB sizes, due to a fast discharge of the LIB. Therefore, a bigger genset or LIB would be required in order to make IPF-CD a feasible strategy. Anyway, this EMS becomes a good option when appropriately combined with IPF-CS (what is done in SM and GA-SM strategies), as it is discussed below.

DP is the EMS that obtains the best result with LTO and NMC technologies, as it is able to reduce the LCC of a traditional DEMU up to 5.2% and 4.7%, respectively. As the optimised variable is the fuel use, DP is also the EMS with lowest diesel consumption: compared to the DEMU, reductions of the 18.7% (LTO), 25.7% (NMC) and 20.8% (LFP) are achieved. The simulation results depicted in Fig. 14 show a relation between a higher depth of discharge realized by the LIB and a lower diesel use, what demonstrates the importance of designing strategies focused on depleting the charge of the LIB. As DP strategy is hardly applicable in real operation, the obtained results are used to evaluate the performance of the remainder strategies.

Regarding the optimization strategies that can be deployed in a real application, GA-SM obtains the best results. Focusing on the best LIB technologies (LTO and NMC), GA-SM reduces the LCC of a traditional DEMU around 3.6-4.0%, and it is just a 1.3-1.4% ahead of the results of DP strategy. Compared to the other GA-based strategy (GA-FL), the LCC is improved a 0.7% in both cases of NMC and LTO. The SOC profiles of GA-SM strategy depicted in Fig. 14 show that, even if a good result is obtained compared to other EMSs, there is still room to design a control policy that can get closer to the optimal SOC trajectory proposed by DP, specially in the case of NMC technology.

Focusing on the rule-based strategies, IPF-CS and SM obtain the best results. Considering that SM strategy was designed to be more complete than IPF-CS (SOC adaptive strategy), it might have obtained a better result. However, SM only improves the results of IPF-CS in the case of NMC technology (0.2% lower, while in LTO and LFP the LCC is 0.5% and 0.4% higher). This demonstrates the importance of correctly designing the SOC thresholds in SM strategy, which should be adapted to the specific characteristics of each scenario. When optimizing these thresholds (as done in GA-SM), the results of SM are improved a 1.1% (LTO), 0.5% (NMC) and 1.0% (LFP). Therefore, the obtained results highlight the importance of deploying a GA approach for improving the performance of the rule-based SM strategy. Fig. 14 also helps to understand how the improvements proposed by the GA optimization change the control policy, as the SOC profiles of SM and GA-SM strategies are depicted together.

Regarding FL strategy, it can not improve the results of most of the rule-based strategies. Compared to IPF-CS, the LCC is 0.2% (LTO), 0.5% (NMC) and 4.0% (LFP) higher. The result is

specially poor in LFP technology, as the strategy is not able to control the degradation of the LIB. The results demonstrate that not always a more complicated strategy obtains a better result. Even if with the GA optimization the performance is improved compared to the original FL strategy (0.4% in NMC and 2% in LFP, with no improvement in LTO), it cannot outperform the result of GA-SM strategy, as it was previously outlined. Hence, it is concluded that the philosophy proposed in SM is more appropriated than the one proposed in FL.

The strategy with the worst result is found to be PF, which can barely improve the LCC of the traditional DEMU. The main reason is found to be that, compared to the traditional DEMU, similar diesel consumption values are obtained. While in the case with the lowest fuel use (DP with NMC) the diesel reduction is 25.7%, in the cases of PF strategy the reduction just reaches the 3.5% (LTO), 0.7% (NMC), and 1.0% (LFP). It is worth to highlight that, as it was previously outlined, when a strategy is able to reduce the diesel use, a better result is obtained (as long as the degradation is adequately controlled).

In conclusion, it can be stated that optimization strategies obtain the best results. Considering that DP is hardly applicable in a real application, GA-SM is found to be the most appropriated option, obtaining a 3.4-4.0% LCC reduction compared the traditional DEMU when integrating NMC and LTO technologies. Besides, it has been found that when comparing EMSs, the diesel consumption and LIB degradation become the most important terms of the LCC. Finally, the importance of developing a GA optimization approach for obtaining a cost-optimal strategy has also been highlighted.

C. Analysis of Optimal Sizing Results

The analysis of the sizing results for the proposed scenario unveils that the optimal genset sizes are always around 1000-1500 kW (i.e. 2-3 gensets). In short, in LTO technology the optimal size is always 1000 kW, in NMC the option of 1500 kW is only proposed in PF and FL strategies, and in LFP the option of 1000 kW is only proposed in FL and DP strategies. Therefore, considering that LTO and NMC are the technologies that obtain the best results, and that in FL and PF strategies NMC does not obtain a good LCC, it can be concluded that the option of 1000 kW is the most appropriated one for the proposed scenario.

Regarding the installed LIB energy, the results show that in general the optimal solutions are close to the maximum allowable values (Fig. 11). In LTO technology, excluding the result of PF strategy, the optimal LIB sizes are around 300-360 kWh (being the maximum allowable 360 kWh). In NMC technology, in the cases of a big genset (1500 kW) the optimal LIB sizes are between 280-300 kWh (being the maximum allowable 300 kWh), while in the cases of a small genset (1000 kW) the optimal sizes are around 480-600 kWh (being the maximum allowable 600 kWh). Finally, in LFP technology, except in the case of GA-FL (180 kWh), the optimal LIB size is always the maximum allowable energy (200 kWh in the cases of the big genset, and 400 kWh in the cases of the small genset). It is also found that in the cases with lowest diesel use (e.g. in DP strategy), the optimal LIB sizes coincide with the maximum allowable energy values.

In conclusion, it can be stated that in the proposed scenario, as long as an appropriate LIB technology is selected and an adequate strategy is designed, the optimal sizing results are close to a genset of 1000 kW and the maximum allowable LIB size (360 kWh in LTO, 600 kWh in NMC and 400 kWh in LFP). The results enforce the idea that as much energy is harnessed from the LIB (both by integrating big LIB systems and designing strategies oriented to deplete its charge), a better LCC is obtained.

VII. Conclusion

This paper has analysed the influence of the EMS, the LIB technology and the size of the power sources on the LCC of railway projects involving H-DEMUs. A sensitivity analysis composed of 24 cases has been proposed, focused on 8 EMSs (including rule-based and optimization-based strategies) and 3 LIB technologies (NMC, LTO and LFP). In order to develop the analysis, a methodology has been presented, which returns the LCC value and the optimal genset and LIB sizes for each case of the sensitivity analysis. The methodology has been implemented in a scenario based on a real railway line. This approach is found to be potentially helpful for the cost-optimal design (technologies and size selection) and operation definition (EMS) of powertrains for hybrid diesel-electric railway vehicles.

The techno-economical analysis of the results has lead to several conclusions. Regarding the analysis of the LIB technologies, LTO and NMC have been found to be the most appropriated options for the proposed application, thanks to their lower replacement costs compared to LFP. Besides, the analysis of the EMSs has highlighted the importance of implementing GA optimization approaches that improve the performance of typical rule-based strategies. GA-SM has been found to be the most appropriate strategy for the proposed application, obtaining a LCC reduction around the 3.4-4.0% compared to a traditional DEMU. Anyway, it has been identified that further improvements can be potentially obtained if a rule-based strategy is designed focused on replicating the optimal control policy proposed by the DP approach. Finally, regarding the sizes of the power sources, it has been found that the optimal design is close to a genset of 1000 kW and the maximum allowable LIB size (which depends on the LIB technology). In short, the analysis has highlighted the importance of harnessing as much energy as possible from the LIB, both by integrating big battery systems (e.g. in NMC chemistry) or by designing strategies oriented to deplete its charge (e.g. in LTO chemistry).

Future developments and improvements of this work may consider rule-based strategies designed with the aim of replicating the optimal control policies proposed by the DP approach. An extension of the LCC analysis in order to consider scenarios with different characteristics is also proposed, in order to extend the obtained conclusions to more case studies. Finally, this study can be replicated with other topologies such as the FC-based railway vehicle.

ACKNOWLEDGMENT

The authors would like to thank CAF Power and Automation for their support in the course of this investigation.

REFERENCES

[1] C. Wu, B. Xu, S. Lu, F. Xue, L. Jiang, and M. Chen, "Adaptive eco-driving strategy and feasibility analysis for electric trains with on-board energy storage devices," *IEEE Trans. Transp. Electrific.*, vol. 7, no. 3, pp. 1834–1848, Sep. 2021, doi: 10.1109/TTE.2021.3050470.

[2] International Energy Agency (IEA) and International Union of Railways (UIC), "Railway handbook 2017," IEA, Paris, France, Tech. Rep. 6, Nov. 2017.

[3] A. Jaafar, C. Akli, B. Sareni, X. Roboam, and A. Jeunesse, "Sizing and energy management of a hybrid locomotive based on flywheel and accumulators," *IEEE Trans. Veh. Technol.*, vol. 58, no. 8, pp. 3947–3958, Oct. 2009, doi: 10.1109/TVT.2009.2027328.

[4] F. Zenith, R. Isaac, A. Hoffrichter, M. S. Thomassen, and S. Møller-Holst, "Techno-economic analysis of freight railway electrification by overhead line, hydrogen and batteries: Case studies in Norway and USA," *Proc. Inst. Mech. Engineers, Part F, J. Rail Rapid Transit*, vol. 234, no. 7, pp. 791–802, Aug. 2020, doi: 10.1177/0954409719867495.

[5] J. Pagenkopf and S. Kaimer, "Potentials of alternative propulsion systems for railway vehicles - A techno-economic evaluation," in *Proc. 9th Int. Conf. Ecological Veh. Renewable Energies*, 2014, pp. 1–8, doi: 10.1109/EVER.2014.6843995.

[6] C. Wu, S. Lu, F. Xue, L. Jiang, and M. Chen, "Optimal sizing of onboard energy storage devices for electrified railway systems," *IEEE Trans. Transp. Electrific.*, vol. 6, no. 3, pp. 1301–1311, Sep. 2020, doi: 10.1109/TTE.2020.2996362.

[7] Z. Zhong, Z. Yang, X. Fang, F. Lin, and Z. Tian, "Hierarchical optimization of an on-board supercapacitor energy storage system considering train electric braking characteristics and system loss," *IEEE Trans. Veh. Technol.*, vol. 69, no. 3, pp. 2576–2587, Mar. 2020, doi: 10.1109/TVT.2020.2967467.

[8] A. González-Gil, R. Palacin, and P. Batty, "Sustainable urban rail systems: Strategies and technologies for optimal management of regenerative braking energy," *Energy Convers. Manage.*, vol. 75, no. 75, pp. 374–388, Nov. 2013, doi: 10.1016/j.enconman.2013.06.039.

[9] A. Kumar and M. Sehgal, "Hydrogen fuel cell technology for a sustainable future: A review," in *SAE Tech. Papers*, vol. 2018, pp. 1–11, 2018.

[10] International Energy Agency (IEA), "The future of hydrogen," IEA, Paris, France, Tech. Rep. 1, Jun. 2019.

[11] K. Turcheniuk, D. Bondarev, G. G. Amatucci, and G. Yushin, "Battery materials for low-cost electric transportation," *Mater. Today*, vol. 42, no. February, pp. 57–72, Jan. 2021, doi: 10.1016/j.mattod.2020.09.027.

[12] M. A. Hannan, M. M. Hoque, A. Hussain, Y. Yusof, and P. J. Ker, "State-of-the-art and energy management system of lithium-ion batteries in electric vehicle applications: Issues and recommendations," *IEEE Access*, vol. 6, pp. 19 362–19 378, 2018, doi: 10.1109/ACCESS.2018.2817655.

[13] Y. Ruf *et al.*, "Study on the use of fuel cells and hydrogen in the railway environment," Roland Berger, Luxembourg, Tech. Rep. HI-02-19-229-EN-C, Apr. 2019.

[14] V. I. Herrera, H. Gaztanaga, A. Milo, A. Saez-de Ibarra, I. Etxeberria-Otadui, and T. Nieva, "Optimal energy management and sizing of a battery-supercapacitor-based light rail vehicle with a multiobjective approach," *IEEE Trans. Ind. Appl.*, vol. 52, no. 4, pp. 3367–3377, Jul. 2016, doi: 10.1109/TIA.2016.2555790.

[15] C. Zhai, F. Luo, and Y. Liu, "A novel predictive energy management strategy for electric vehicles based on velocity prediction," *IEEE Trans. Veh. Technol.*, vol. 69, no. 11, pp. 12 559–12 569, Nov. 2020, doi: 10.1109/TVT.2020.3025686.

[16] Z. Xin and T. Yi, "Research of hybrid electric locomotive control strategy," *Proc. Int. Conf. Syst. Sci., Eng. Des. Manuf. Informatization*, vol. 1, pp. 118–122, 2011.

[17] C. Lanneluc, J. Pouget, M. Poline, F. Chauvet, and L. Gerbaud, "Optimal energy management of a hybrid train: Focus on saving braking energy," *Proc. IEEE Veh. Power Propulsion Conf.*, vol. 2018, pp. 1–6, 2017, doi: 10.1109/VPPC.2017.8330927.

[18] M. Leska, H. Aschemann, M. Melzer, and M. Meinert, "Comparative calculation of the fuel-optimal operating strategy for diesel hybrid railway vehicles," *Int. J. Appl. Math. Comput. Sci.*, vol. 27, no. 2, pp. 323–336, Jun. 2017, doi: 10.1515/amcs-2017-0023.

[19] H. Shibuya and K. Kondo, "Designing methods of capacitance and control system for a diesel engine and EDLC hybrid powered railway traction system," *IEEE Trans. Ind. Electron.*, vol. 58, no. 9, pp. 4232–4240, Sep. 2011, doi: 10.1109/TIE.2010.2100332.

[20] M. Poline, L. Gerbaud, J. Pouget, and F. Chauvet, "Simultaneous optimization of sizing and energy management-application to hybrid train," *Math. Comput. Simul.*, vol. 158, pp. 355–374, Apr. 2019, doi: 10.1016/j.matcom.2018.09.021.

[21] A. Mirabadi and M. Najafi, "Energy management system in hybrid trains using fuzzy control: A comparative study," *Proc. Inst. Mech. Engineers, Part F, J. Rail Rapid Transit*, vol. 225, no. 3, pp. 267–276, May 2011, doi: 10.1243/09544097JRRT397.

[22] M. Sorrentino, K. Serge Agbli, D. Hissel, F. Chauvet, and T. Letrouve, "Application of dynamic programming to optimal energy management of grid-independent hybrid railcars," *Proc. Inst. Mech. Engineers, Part F, J. Rail Rapid Transit*, vol. 235, no. 2, pp. 236–247, 2021, doi: 10.1177/0954409720920080.

[23] M. Leska, R. Prabel, A. Rauh, and H. Aschemann, "Simulation and optimization of the longitudinal dynamics of parallel hybrid railway vehicles," in *FORMS/FORMAT 2010*. Berlin, Heidelberg: Springer, 2011, pp. 155–164, doi: 10.1007/978-3-642-14261-1_16.

[24] J. Baert, S. Jemei, D. Chamagne, D. Hissel, S. Hibon, and D. Hegy, "Energetic macroscopic representation and optimal fuzzy logic energy management strategy of a hybrid electric locomotive with experimental characterization of nickel-cadmium battery cells," *EPE J.*, vol. 24, no. 4, pp. 56–67, Dec. 2014, doi: 10.1080/09398368.2014.11755459.

[25] Y. Yan, Q. Li, W. Chen, B. Su, J. Liu, and L. Ma, "Optimal energy management and control in multimode equivalent energy consumption of fuel cell/supercapacitor of hybrid electric tram," *IEEE Trans. Ind. Electron.*, vol. 66, no. 8, pp. 6065–6076, Aug. 2019, doi: 10.1109/TIE.2018.2871792.

[26] Z. Jia, J. Jiang, H. Lin, and L. Cheng, "A real-time MPC-based energy management of hybrid energy storage system in urban rail vehicles," *Energy Procedia*, vol. 152, pp. 526–531, Oct. 2018, doi: 10.1016/j.egypro.2018.09.205.

[27] J. Olmos, I. Gandiaga, A. Saez-de Ibarra, X. Larrea, T. Nieva, and I. Aizpuru, "Modelling the cycling degradation of li-ion batteries: Chemistry influenced stress factors," *J. Energy Storage*, vol. 40, no. June, Aug. 2021, Art. no. 102765, doi: 10.1016/j.est.2021.102765.

[28] C. Depature and T. Letrouvé, "Innovative train technologies energy comparison on one non electrified railway," in *Proc. IEEE Veh. Power Propulsion Conf.*, Gijón, 2020, pp. 1–6, doi: 10.1109/VPPC49601.2020.9330938.

[29] M. Cipek, D. Pavković, Z. Kljaić, and T. J. Mlinarić, "Assessment of battery-hybrid diesel-electric locomotive fuel savings and emission reduction potentials based on a realistic mountainous rail route," *Energy*, vol. 173, pp. 1154–1171, Apr. 2019, doi: 10.1016/j.energy.2019.02.144.

[30] R. Giglioli, G. Lutzemberger, D. Poli, and L. Sani, "Hybridisation of railcars for usage in non-electrified lines," in *Proc. 6th Int. Conf. Clean Elect. Power*, 2017, pp. 525–530, doi: 10.1109/ICCEP.2017.8004738.

[31] M. Meinert, M. Melzer, C. Kamburow, R. Palacin, M. Leska, and H. Aschemann, "Benefits of hybridisation of diesel driven rail vehicles: Energy management strategies and life-cycle costs appraisal," *Appl. Energy*, vol. 157, pp. 897–904, Nov. 2015, doi: 10.1016/j.apenergy.2015.05.051.

[32] M. Meinert, P. Prenleloup, S. Schmid, and R. Palacin, "Energy storage technologies and hybrid architectures for specific diesel-driven rail duty cycles: Design and system integration aspects," *Appl. Energy*, vol. 157, no. 2015, pp. 619–629, 2015, doi: 10.1016/j.apenergy.2015.05.015.

[33] Construcciones y Auxiliar de Ferrocarriles (CAF)2, "CIVITY, a family of trains for commuter and regional services," 2020, Accessed: Sep. 16, 2021. [Online]. Available: https://www.caf.net/en/productos-servicios/familia/civity/index.php

[34] M. Mabrey, "Advantages and marine applications of various lithium ion battery chemistries," in *Proc. MARAD META Battery Propulsion Conf.*, 2016, pp. 1–18.

[35] J. A. López-Ibarra, N. Goitia-Zabaleta, V. I. Herrera, H. Gaztañaga, and H. Camblong, "Battery aging conscious intelligent energy management strategy and sensitivity analysis of the critical factors for plug-in hybrid electric buses," *eTransportation*, vol. 5, Aug. 2020, Art. no. 100061, doi: 10.1016/j.etran.2020.100061.

[36] O. Sundstrom and L. Guzzella, "A generic dynamic programming Matlab function," in *IEEE Control Appl.*, (*CCA) Intell. Control*, 2009, pp. 1625–1630.

[37] J. A. López-Ibarra, H. Gaztañaga, A. Saez-de Ibarra, and H. Camblong, "Plug-in hybrid electric buses total cost of ownership optimization at fleet level based on battery aging," *Appl. Energy*, vol. 280, no. August, Dec. 2020, Art. no. 115887, doi: 10.1016/j.apenergy.2020.115887.

[38] A. Lajunen and T. Lipman, "Lifecycle cost assessment and carbon dioxide emissions of diesel, natural gas, hybrid electric, fuel cell hybrid and electric transit buses," *Energy*, vol. 106, pp. 329–342, Jul. 2016, doi: 10.1016/j.energy.2016.03.075.

Josu Olmos received the B.Sc. degree in renewable energies engineering and the M.Sc. degree in control in smart grids and distributed generation from the University of the Basque Country, UPV/EHU, Spain, in 2017 and 2018, respectively. In 2018, he joined IKERLAN Technology Research Centre (BRTA), Arrasate-Mondragón, Spain, where he is currently working toward the Ph.D. degree with the Energy Storage and Management Department and in collaboration with the University of Mondragón, Mondragón, Spain. His research interests include the integration of energy storage technologies in mobility applications, in particular on the development of optimal energy management strategies.

Iñigo Gandiaga received the Diploma in physics from the University of the Basque Country, UPV/EHU, Spain, in 2010. He joined the Energy Business Unit of IKERLAN Technology Research Centre (BRTA) in 2010. His research interests include lifetime estimation and sizing studies of different electrochemical energy storage technologies (EDLC, Li-ion and NiMH) for heavy duty transport and stationary applications to SOC/SOH estimation algorithms for lithium-ion battery management systems. He is a Co-Ordinator of various research projects with different industrial partners such as CAF or General Electric.

Dimas Lopez received the B.Sc. degree in electronic engineering from the University of the Basque Country, UPV/EHU, Spain, in 2000, the M.Sc. degree in electronic engineering from the University of Navarra - TECNUN, Spain, and the Ph.D. degree in mechanical engineering from the same institution in 2003 and 2010, respectively. He joined CAF P&A in 2011 as SW Engineer in the early projects of catenary-free tramways. He currently works as an ESS Product Development Manager for rolling stock vehicles combining different disciplines including SW, power electronics or electromechanics.

Xabier Larrea received the B.Sc. degree in electronic engineering from the University of Mondragon, Mondragón, Spain, in 2004, the M.Sc. degree in electrical and electronics engineering from Ecole Polytechnique Fédérale de Lausanne, Switzerland, in 2007, and an Executive MBA from Deusto Business School, Spain, in 2018. He joined CAF P&A in 2010 as a Project Manager for locomotive and catenary-free tramway projects. He is currently a Technical Manager of ESS products and is responsible of the development and life cycle management of ESS products for different rolling stock vehicles.

Txomin Nieva received the Diploma in system engineering from the University of Mondragon, Mondragón, Spain, in 1997 and the Ph.D. degree in computer Science from the Ecole Polytechnique Fédérale de Lausanne, Switzerland, in 2001. In 2004, he joined the CAF Group. He is currently the Chief Technology Officer (CTO) of CAF's subsidiary company CAF P&A, where he moved to in 2007. He Leads a large group of research engineers in power electronics, electromechanical design, control electronics and SW areas. He is responsible for developing new products for propulsion systems, control & communication systems, and ESS.

Iosu Aizpuru received the B.Sc, M.Sc., and Ph.D. degrees in electrical engineering from the University of Mondragon, Mondragón, Spain, in 2006, 2009, and 2015, respectively. He is currently a Researcher and Lecturer with the Department of Electronics, Faculty of Engineering. His current research interests include power electronics modeling, energy storage modeling and control of energy storage systems via power electronic converters. He has participated in various research projects in the fields of traction and stationary systems for railway applications, renewable energy applications and energy storage applications for traction, on-grid, and off-grid systems.